

INSTITUT TEHNIČKIH NAUKA SANU

Knez Mihailova 35/IV

Beograd

Predmet: Zahtev za pokretanje postupka za izbor dipl.ing. Vesne Lojpur, istraživaca
pripravnika u zvanje istraživač saradnik

NAUČNOM VEĆU INSTITUTA TEHNIČKIH NAUKA SANU

Molim Vas da, u skladu sa Pravilnikom o postupku i načinu vrednovanja, i kvantitativnom iskazivanju naučnoistraživačkih rezultata istraživača (Sl. Glasnik RS, br. 38/08), i Pravilnikom o sticanju zvanja istraživač saradnik, Naučno veće Instituta tehničkih nauka SANU pokrene postupak za moj izbor u zvanje istraživač saradnik.

Za članove komisije za pripremu izveštaja Naučnom Veću predlažem:

- dr Oliveru Milošević, naučnog savetnika Instituta tehničkih nauka SANU
- dr Lidiju Mančić, višeg naučnog saradnika Instituta tehničkih nauka SANU
- dr Smilja Marković, naučnog saradnika Instituta tehničkih nauka SANU

U prilogu dostavljam:

1. biografiju
2. dokaz o upisanim doktorskim studijama
3. dokaz o ukupnoj prosečnoj oceni na osnovnim studijama
4. bibliografiju sa kopijama rada

U Beogradu

22. 2. 2012.

Podnosilac zahteva

Vesna Lojpur

Vesna Lojpur, dipl.ing

Istraživač pripravnik ITN SANU

Биографија Весна Лојпур

Весна Лојпур рођена је 16.03 1984. године у Мостару, Босна и Херцеговина. Основне студије је уписала школске 2002/03 године на Технолошко-металуршком факултету у Београду и завршила их је 2009. године са просечном оценом 8.79 и 10 на дипломском раду „ Испитивање услова добијања некохерентних снопова оптичких влакана“. Постдипломске докторске студије је уписала 2009. године, на истом факултету на катедри за Конструкционе и специјалне материјале. Тренутно је на трећој години студија.

У Институту техничких наука САНУ је запослена од 2009. године као истраживач приправник. Ангажована је на пројектима основних истраживања ОИ172035 „Рационални дизајн и синтеза биолошки активних и координационих једињења и функционалних материјала , релевантних у (био) нанотехнологији“ и на пројекту интегралних и интердисциплинарних истраживања ИИИ45020, „Материјали редуковане димензионалности за ефикасну апсорпцију светлости и конверзију енергије“.

Области интересовања су јој синтеза и карактеризација наноструктурних материјала добијених методом спреј пиролизе и хидротермалном методом, опто-електронски и упконверторски материјли.

Библиографија Весна Лојпур

М 21 Врхунски међународни часопис

1. Lidija Mancic, Vesna Lojpur, Maria Eugenia Rabanal and Olivera Milosevic, Synthesis of fine YAP:Ce phosphor particles *via* aerosol route, European Journal of Inorganic Chemistry, DOI 10.1002/ejic.200

М 33 Међународни зборник саопштења штампан у целини

1. V.Lojpur, K.Marinkovic, L. Mancic,M.E. Rabanal, L.S.Gomez, J.M.Torralba,O. Milosevic,Nanostructured luminiscence particles synthesized through aerosol route at intermediate temperature, Slanic-Moldova, Romania,2010, Proceedings of the ModTech, ISSN 2066–3919 , 355–358

М 34 Међународни зборник саопштења штампан у изводу

1. Vesna Lojpur, Katarina Marinković, Lidija Mančić, Luz Gomes, Maria Eugenia Rabanal, Olivera Milošević, Effect of Dopants on Structural and Morfological Characteristic of Phosphors Particles Synthesised through Spray Pyrolysis, IMANAM 2010, 4–9 July 2010, Zurich, Switzerland
2. Ivan Dugandžić, Vesna Lojpur, Lidija Mančić, Maria Eugenia Rabanal,Olivera Milošević, Dense spherical rare earth oxide particles synthesis via spray pyrolysis of polymeric precursor solution, YUCOMAT 2010, 6–10 September, 2010, Herceg-Novi, Montenegro,Abstract Book, p.92
3. Lidija Mancic, Katarina Marinkovic, Ivan Dugandzic, Vesna Lojpur Olivera Milosevic, Soft chemistry routes for synthesis of 3D and 1D nanostructures, First Conference of the Serbian Ceramic Society, March 17-18 2011, Belgade, Serbia, Abstract Book, p.45
4. V. Lojpur, L. Mancic, Maria Eugenia Rabanal, Olivera Milosevic SYNTHESIS OF THE NANOSTRUCTURED YAP:Ce *VIA* SPRAY PYROLYSIS BY POLYMERIC PRECURSOR SOLUTION, Yucomat, September 5-9,2011 Herceg Novi, Montenegro, Abstract Book p.97
5. Lidija Mancic, Vesna Lojpur, Maria Eugenia Rabanal and Olivera Milosevic, Synthesis of fine YAP:Ce phosphor particles *via* aerosol route, Abstract Book
6. V. Lojpur, L. Mancic , Maria Eugenia Rabanal, Miroslav Dramicanin, Olivera Milosevic Influence of thermal treatment on structural, morphological and optical characteristics of upconvertors, Tenth Young Researchers' Conference-Material Science and Engineering 2011, SANU, Belgrade December 21-23, In Press
7. Ivan Dugandžić, Vesna Lojpur, Katarina Marinkovic, Lidija Mančić, Maria Eugenia Rabanal, Olivera Milošević, NANOPHOSPHORS SYNTHESIS THROUGH SOLVOTHERMAL ROUTE, ModTech May 25-27 2011, Vadul lui Voda-Chisinau, Republic of Moldova, Abstract Book p. 369

РЕПУБЛИКА СРБИЈА



УНИВЕРЗИТЕТ У БЕОГРАДУ
ТЕХНОЛОШКО - МЕТАЛУРШКИ ФАКУЛТЕТ

ДИПЛОМА

О СТЕЧЕНОМ ВИСОКОМ ОБРАЗОВАЊУ

ВЕСНА (Миле) ЛОЈПУР

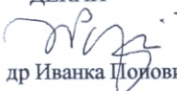
РОЂЕНА 16. МАРТА 1984. ГОДИНЕ У МОСТАРУ, РЕПУБЛИКА БОСНА И ХЕРЦЕГОВИНА, УПИСАНА ЈЕ 2002/03. ШКОЛСКЕ ГОДИНЕ, А ДАНА 16. МАРТА 2009. ГОДИНЕ ЗАВРШИЛА ЈЕ СТУДИЈЕ НА ТЕХНОЛОШКО-МЕТАЛУРШКОМ ФАКУЛТЕТУ, ОДСЕК - **ИНЖЕЊЕРСТВО МАТЕРИЈАЛА**, СА ОПШТИМ УСПЕХОМ 8,79 (ОСАМ И 79/100) У ТОКУ СТУДИЈА И ОЦЕНОМ 10 (ДЕСЕТ) НА ДИПЛОМСКОМ ИСПИТУ.

НА ОСНОВУ ТОГА ИЗДАЈЕ ЈОЈ СЕ ОВА ДИПЛОМА О СТЕЧЕНОМ ВИСОКОМ ОБРАЗОВАЊУ И СТРУЧНОМ НАЗИВУ

ДИПЛОМИРАНИ ИНЖЕЊЕР ТЕХНОЛОГИЈЕ

Редни број из евиденције о издатим дипломама 9696

У Београду, 16. марта 2009. године

ДЕКАН

Проф. др Иванка Лојдовић

РЕКТОР

Проф. др Бранко Ковачевић



Република Србија
Универзитет у Београду
Технолошко-металуршки факултет
Д.Бр.5
Датум: 20.12.2011. године

На основу члана 161 Закона о општем управном поступку и службене евиденције издаје се

УВЕРЕЊЕ

Лојпур (Миле) Весна, бр. индекса 2009/4010, рођена 16.03.1984. године, Мостар, Босна и Херцеговина, уписана школске 2011/2012. године, у статусу: самофинансирајући; тип студија: Докторске академске студије; студијски програм: Инжењерство материјала 08.

Према Статуту факултета студије трају (број година): три године.
Рок за завршетак студија: у двоструком трајању студија.

Ово се уверење може употребити за регулисање војне обавезе, издавање визе, права на дечији додаток, породичне пензије, инвалидског додатка, добијања здравствене књижице, легитимације за повлашћену вожњу и стипендије.



Овлашћено лице факултета

[Handwritten signature]

Synthesis of cerium activated yttrium aluminate-based fine phosphors via aerosol route

Lidija Mancic,^[a] Vesna Lojpur,^[a] Ignacio Barosso^[b], Maria Eugenia Rabanal^[b] and Olivera Milosevic^{*[a]}

Keywords: Yttrium aluminates / Nanoparticles/ Luminescence / Polymerization / Spray pyrolysis /

Polycrystalline yttrium aluminate-based fine powders doped with Ce³⁺ were synthesized via spray pyrolysis of the polymeric precursor obtained by dissolving the corresponding nitrates in EDTA/EG solution. Aerosol decomposition was performed at 550 °C followed by additional thermal treatment (900-1100 °C). Obtaining of either single YAP or YAG phase was investigated as a function of predefined yttrium to aluminium ratio, cerium doping concentration, processing temperature and the thermal treatment regime, including changeable heating/cooling rates (dT/dt), residence time (t) and atmosphere. Changes in precursor composition and structure during thermal decomposition were investigated by TGA/DTA and FTIR spectroscopy. The particle morphology and structure were analyzed by scanning electron microscopy (SEM/EDS) and transmission electron microscopy (HR-TEM). Phase identification was performed by X-ray powder diffraction (XRPD) on which bases the structural refinement was

done. The emission spectra were recorded within the range of 325-800 nm, by application of excitation wavelength of 297 nm (YAP) and 450 nm (YAG). The employed synthesis conditions assured formation of spherical, non-agglomerated particles, with well developed surfaces, ranging between 200 to 800 nm. For predefined Y:Al ratio of 1, lower processing temperatures combined with longer heat treatments in stationary conditions resulted in the multi-phase system, composed of YAP, YAG and YAM mixture phases. However, short heat treatment at higher temperature, associated with high heating rate (200 °/min) results in a pure kinetically favoured YAP hexagonal phase formation. On the other hand, for predefined Y:Al ratio of 3:5, the generation of a pure thermodynamically stable YAG phase has been confirmed, regardless applied heat treatment conditions. Although incomplete, Ce³⁺ introduction into the host matrix, has been detected by XRPD and luminescence measurements.

Introduction

Trivalent cerium activated yttrium aluminates have undergone extensive research for different display applications in electronics and optoelectronics, due to their efficient luminescence properties, good thermal, mechanical and chemical stability.^[1-3] As for system phases, yttrium aluminum garnet (YAG:Ce³⁺), has been found to be a suitable material for non-polluting production of high energy-efficiency white light.^[2] Moreover, yttrium aluminum perovskite (YAP) represents a suitable host phosphor material for microwave and high frequency applications due to its low dielectric constant.^[3] In addition, both cerium-doped YAP and YAG, represent promising fast scintillators for synchrotron X-ray experiments and they are suitable for applications relating to medical imaging, such as PET, SPET, gamma-ray camera etc.^[4-7]

These systems have been described in literature in three different kinds of crystal phases:^[8,9] yttria-alumina perovskites, yttria alumina garnets and monoclinic with yttrium to aluminum ratio as presented in Table 1. Yttria-alumina perovskite has three kinetically favoured forms: hexagonal, orthorhombic and cubic. Literature records suggest that great many materials exhibit orthorhombic *Pnma* distorted structure and a hexagonal *P63cm* form as well; the latter practically loses its similarity with perovskite symmetry due to a high distortion level. This phase has been found exclusively in chemically synthesized powders.^[9,10] The yttria-alumina perovskites, YAP, represent the metastable forms in the yttria-alumina system, commonly formed jointly with stable YAG and YAM phases due to the reaction of dissociation:



The crystallography of cubic garnet, Y₃Al₅O₁₂, having *Ia-3d* space group, can be explained as a disordered close packed array of oxygen of isometric symmetry, forming AlO₆ octahedra and AlO₄ tetrahedra, with Y³⁺ ions in AO₈ dodecahedron^[11]. The Y³⁺ ions could be partially substituted by rare-earth (RE) ions.

[a] Institute of Technical Sciences of SASA
Knez Mihailova 35/IV, 11000 Belgrade, Serbia
Fax: +381112185263
E-mail: olivera.milosevic@itn.sanu.ac.rs

[b] Dept. of Materials Science and Engineering and Chemical Engineering, University Carlos III of Madrid,
Avd. Universidad 30, 28911 Leganes, Madrid, Spain

Supporting information for this article is available on the WWW under <http://www.eurjic.org/>

Table 1. Crystal phases in Y_2O_3 - Al_2O_3 system

Crystal phase formula	Y:Al	Crystal structure/symmetry
Perovskite, YAP: $YAlO_3$	1:1	Cubic Orthorhombic, $Pnma$ (or $Pbnm$) Hexagonal (P_63cm)
Garnet, YAG: $Y_3Al_5O_{12}$	3:5 (or 0.6:1)	Cubic, $Ia-3d$
YAM: $Y_4Al_2O_9$	(2:1)	Monoclinic Orthorhombic

Pure phase synthesis in yttria-alumina system is very hard to achieve, even through soft chemistry routes and still makes a challenge since the formation of other phases occurs simultaneously. The yttria-alumina phase diagram^[12,13] in which the ratio of 2:1 refers to the formation of monoclinic $Y_4Al_2O_9$ and 3:5 refers to the formation of garnet $Y_3Al_5O_{12}$, evidences that the structure of the compositions is not straightforward one and the equilibrium reaction (Eq.1) leads rather to the dissociation than to formation of the multi-phase system.

In comparison to conventional solid-state processing, in which high temperatures and long residence time are necessary, current phosphor materials are usually produced via soft-chemistry routes, enabling many advantages with regard to their structural and morphological features. Anticipating that nanostructuring will enable prosperous future development of optical devices perceived through high brightness, reliability, low power consumption and a long life of phosphor materials, various efficient wet-chemical synthesis routes have been developed, including sol-gel,^[14] combustion processing,^[15,16] co-precipitation method,^[17] hydrothermal synthesis,^[18,19] etc.

Aerosol route (spray pyrolysis-SP) is an effective, direct method intended to provide nanostructured particles with spherical morphology, agglomerate-free, with a good crystallinity and uniform distribution of a luminescent centre in the host material that consequently contributes to the improvement of optical characteristics of materials.^[20,21] SP is encountered with extreme synthesis conditions occurring at the level of a micrometer sized aerosol droplet in a disperse system thus enabling the synthesis of metastable structures, as previously reported.^[21,22] There are certain process parameters such as high heating/cooling rates, short residence time and post thermal treatment which may affect the obtaining either thermodynamically (YAG, YAM) or kinetically stable phases (YAP).^[12] The introduction of organic components into the solution is ever increasing since they provide the proper retention of stoichiometry during the process and the reaction, occurring in the solution leading to the volume precipitation and the formation of dense particles. Pure YAP phase is already obtained through classical sol gel route but obtained particles are of irregular shape and size due to the extensive agglomeration.^[23-27]

In our previous work we presented synthesis of pure $YAG:Ce^{3+}$ with the spherical shape and filled morphology from the polymeric precursor solution consisting ethylenediaminetetraacetic acid (EDTA) and ethylene glycol (EG).^[28] Further on to our previous research, this paper is to explore controlled aerosol synthesis of pure phosphor particles in yttria-alumina system, as a function of processing parameters and additional thermal treatment regime, including changeable heating/cooling rates (dT/dt), residence time (t) and atmosphere.

Results and Discussion

Polymer precursor: Differential and thermogravimetric thermal analyses (DTA/TGA) were completed in order to determine the mechanism of polymeric precursor decomposition, Figure 1. The first dehydration –related weight loss (~12 wt.-%) occurs at the temperatures up to 200 °C, accompanied with more striking sharper weight change (~32 wt.-%) in the TG curve associated with the CO_2 and NO_x release. Several peaks between 290 and 505 °C indicate bond breaking in the organic and nitrates compounds. In accordance to the literature pure EDTA decomposes endothermically at the temperature ranging between 220 and 280 °C in one step while ignition of its derivatives (exothermic) was initiated at the temperature of about 500 °C. Pure ethylene glycol would present a strong endothermic peak as a result of boiling at 200 °C.^[29] As already pointed out, decomposition of common yttrium and aluminum nitrate precursor is an endothermic process occurring in several steps, at the temperatures between 150 and 400 °C; the most intense are peaked at 200 °C and 390 °C.^[30] Figure 1 leads to the conclusion that herein referred steps overlap with organic phase decomposition resulting in massive removal of gases (~ 44 wt.-%) up to 600 °C. Final loss of volatile compounds from polymeric precursor is registered at 760 and 850 °C (~ 8 wt.-%); aftermath the crystallization of YAP phase is indicative at the temperature of 1100 °C.^[31]

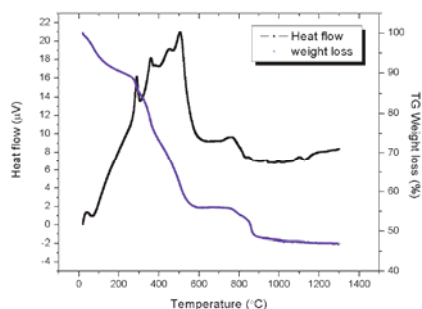


Figure 1. DTA and TGA curves for YAP polymeric precursor

The changes in the precursors composition and structure with the heating is followed by the Fourier transform infrared emission spectroscopy (FTIR). Figure 2 shows FTIR spectra of YAG dried precursors with and without polymers addition, as well as of powder obtained from polymeric one. The intense and wide band peaked at 3360 cm^{-1} in pure nitrate precursor, originates from OH stretching vibration, and its intensity decreases with the addition of EDTA and EG, implying the formation of hydrogen bonds among them.^[32] The vibrations of NO_3^- result in appearance of several peaks in spectral region, ranging from 800 to 1400 cm^{-1} ,^[33] while characteristic stretching of the N-O is reflected as a strong absorption at 1482 cm^{-1} in pure nitrate precursor.^[34] In both precursors, bending vibrations of H_2O are clearly noticeable at 1632 cm^{-1} . EDTA effect on the synthesis process from polymer precursor is indicative one subject to the appearance of metal complexed COO^- asymmetric (at $\sim 1600\text{ cm}^{-1}$) and symmetric (at $\sim 1530\text{ cm}^{-1}$) stretches bands, while esterification process provoked by EG is verified by the appearance of asymmetric stretching modes at 1093 cm^{-1} and 1338 cm^{-1} referring to C-O-C and =C-O-C groups respectively.^[35] These modes become more pronounced with the increase of the temperature and are presented magnified as an inset in Figure 2. As confirmed later on, designated cross-linking of chemical bonds in polymeric precursor, by XRD and TEM analyses, resulted in a pure YAG phase; namely, in powder obtained from YAG polymeric precursor only vibration characteristic for YAG structure, i.e. for Y-O in tetrahedral and Al-O in octahedral arrangements appears at 785 , 720 , 685 , 566 , 448

and 425 cm^{-1} .^[36] Absorption bend of physically adsorbed CO_2 is also visible at 2360 cm^{-1} , while characteristic bends related to mentioned organic groups completely disappear.

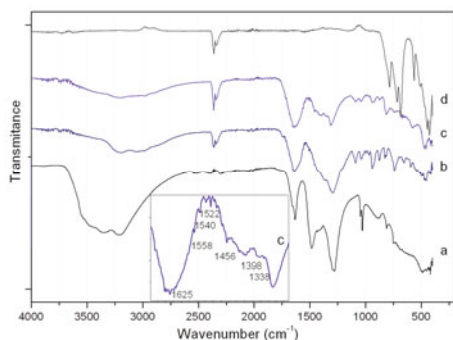


Figure 2 FTIR spectra of YAG: a) pure nitrate precursor dried at $150\text{ }^\circ\text{C}$ b) polymer precursor dried at $150\text{ }^\circ\text{C}$ c) polymer precursor charred at $250\text{ }^\circ\text{C}$ d) powder calcined 12h at $1100\text{ }^\circ\text{C}$

The obtained FTIR results imply following mechanism of polymeric precursor transition with the heating. First, due to its strong chelating ability deprotonated H_4EDTA ($\text{C}_{10}\text{H}_{16}\text{N}_2\text{O}_8$) binds M^{3+} by four oxygen atoms from carboxyl groups and two nitrogen atoms. Since reaction is enhanced in the presence of OH^- ions, NH_4OH is usually added to EDTA solution. Proposed binding and the creation of an octahedral, hexadenate structure for aqueous $\text{Me}^{3+}\text{EDTA}^-$ presented at Figure 3, is confirmed in the $(\text{NH}_4)\text{Al}(\text{EDTA})\cdot 2\text{H}_2\text{O}$ solid compound^[37] while it changes to nonadenate structure in $(\text{NH}_4)\text{Y}(\text{EDTA})\cdot 5\text{H}_2\text{O}$ due to additional bonding of Y^{3+} with three oxygen atoms from water.^[38] With the addition of ethylene glycol $\text{C}_2\text{H}_6\text{O}_2$ cross linking should be realised through the formation of the bonds as follows: carboxyl group from complex forms ester configuration with hydroxyl group from EG; nitrogen from complex reacts with hydroxyl group from EG; and $\text{OH}\cdots\text{O}$ bond is formed between complex- originated oxygen of carbonyl group and OH group from EG.^[39] Having this in mind, it is presumed that during successive SPs steps (evaporation-drying-precipitation), the solvent evaporation in droplets will lead to polycondensation of metal chelates, whereby it is promoted volume precipitation and generation of dense particles.

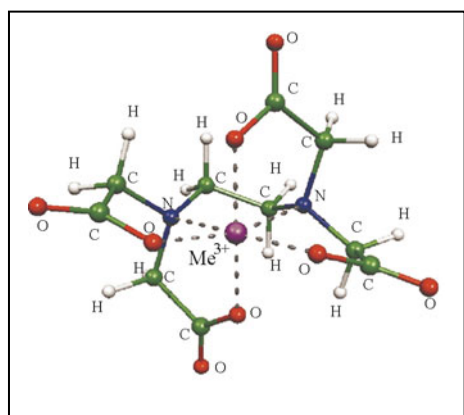


Figure 3 Proposed creation of an octahedral, hexadenate structure for aqueous $\text{Me}^{3+}\text{EDTA}^-$

YAP phase: Synthesized phases in Y-Al-O system (Regime I, doped with 5 at% of Ce), for predefined Y to Al ratio of 1 are identified, on the basis of XRPD data presented in Figure 4. Multi-component powders have been obtained in all cases. The results of Pawley refinements (Table 2) imply changeable phase compositions of powders thermally treated at different temperatures. Prevalence of hexagonal YAP phase (JCPDS 74-1334) is observed at $900\text{ }^\circ\text{C}$, while its orthorhombic modification (JCPDS 89-7947) is detected at higher temperatures. With the temperature rise, the content of the cubic YAG (JCPDS 33-0040) phase increases, while in all samples monoclinic YAM (JCPDS 34-0368) and cubic CeO_2 (JCPDS 81-0792) phases are present as minority ones. Existence of hump (at $2\theta \sim 30^\circ$) indicates retention of amorphous phase in samples. Appearance of cerianite implies incomplete substitution of yttrium with cerium. However, as it will be shown latter, the presence of characteristic green–yellow emission detected in photoluminescence spectra, confirmed the introduction of cerium in the garnet structure. High content of a metastable hexagonal phase in the sample treated at $900\text{ }^\circ\text{C}$, usually appearing in a low content as an intermediate^[9] within narrow temperature frame during synthesis of orthorhombic ones, reveals the possibility for its pure generation via this method. In order to get this kinetically favored phase, higher droplet/particle heating rate was established during aerosol decomposition at $900\text{ }^\circ\text{C}$, while duration of additional thermal treatment is reduced to 1h. XRPD pattern of this sample is shown in Figure 5. The position of the peaks suggests that hexagonal YAP phase was formed without accompany ones from Y-Al-O system. Lattice parameters obtained through Pawley refinement are (in Å): $a=3.675(1)$ and $c=10.515(4)$. The presence of CeO_2 in the powder is indicative due to the appearance of its strongest reflection (110) on two theta 28.54° (marked with * in Figure 5).

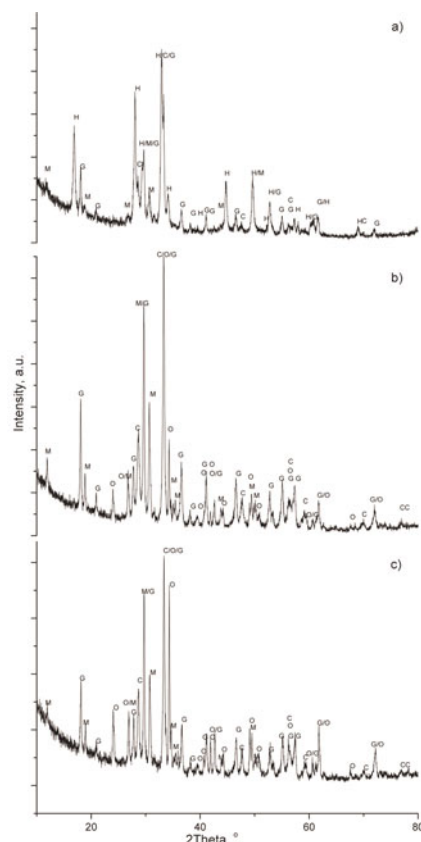


Figure 4. XRPD patterns of Y-Al-O phases synthesized through spray pyrolysis at $550\text{ }^\circ\text{C}$, and subsequent treatment at: $900\text{ }^\circ\text{C}$ (a), $1000\text{ }^\circ\text{C}$ (b), and $1100\text{ }^\circ\text{C}$ (c) for 12h, Regime I (H – YAP hexagonal, O – YAP orthorhombic, G – YAG, M – YAM, C – CeO_2)

Table 2. Microstructural parameters of the phases in Y-Al-O system (doped with 5 at% Ce), synthesized through spray pyrolysis at 550 °C subsequently treated at elevated temperatures for 12 h, Regime I

	900 °C	1000 °C	1100 °C
YAP hex	$a(\text{Å}) = 3.673(1)$		
<i>P63/mmc</i>	$c(\text{Å}) = 10.503(2)$		
	CS(nm)=35(4)		
YAP orthorhombic		$a(\text{Å}) = 5.187(1)$	$a(\text{Å}) = 5.183(1)$
<i>Pbnm</i>		$b(\text{Å}) = 5.326(1)$	$b(\text{Å}) = 5.325(1)$
		$c(\text{Å}) = 7.376(1)$	$c(\text{Å}) = 7.374(1)$
		CS(nm)=269(0)	CS(nm)=215(1)
		Strain(%)=0.09(1)	Strain(%)=0.07(1)
YAG cubic	$a(\text{Å}) = 12.036(1)$	$a(\text{Å}) = 12.043(1)$	$a(\text{Å}) = 12.031(1)$
<i>Ia-3d</i>	CS(nm)=56(0)	CS(nm)=84(9)	CS(nm)=84(9)
YAM monoclinic	Strain(%)=0.29(1)	Strain(%)=0.27(1)	Strain(%)=0.22(1)
<i>P21/a</i>	$a(\text{Å}) = 7.349(4)$	$a(\text{Å}) = 7.385(1)$	$a(\text{Å}) = 7.380(1)$
	$b(\text{Å}) = 10.591(8)$	$b(\text{Å}) = 10.452(1)$	$b(\text{Å}) = 10.446(2)$
	$c(\text{Å}) = 11.037(7)$	$c(\text{Å}) = 11.151(1)$	$c(\text{Å}) = 11.132(2)$
	$\beta(^{\circ}) = 108.25(5)$	$\beta(^{\circ}) = 108.74(1)$	$\beta(^{\circ}) = 108.81(1)$
	CS(nm)=19(7)	CS(nm) = 76(4)	CS(nm)= 73(3)
CeO ₂ cubic	$a(\text{Å}) = 5.499(1)$	$a(\text{Å}) = 5.402(1)$	$a(\text{Å}) = 5.404(1)$
<i>Fm-3m</i>	CS(nm)=18(1)	CS(nm)=18(9)	CS(nm)=29(1)

Information regarding particle morphology and chemical composition are obtained on the basis of SEM and EDS analyses, Figures 6, 7. In all cases, there were obtained highly spherical loosely agglomerated particles, the size of which varied from 200-800 nm. It is clear that low temperature processing at 550 °C, followed by long heat treatment (12h) at higher temperatures (900-1100 °C) ensure generation of particles with high specific surface (Regime I). Primary nanosized subunits, formed through volume precipitation in droplet during spray pyrolysis process form spongy-like surface after powder heating at 900 °C (Figure 6a). With the increase of the temperature, the grained-like particle surface is more pronounced, porosity is noticeably higher and sporadically entirely separated primary particles were recognized in the samples (Figure 6b, c). However, processing at higher temperature (900 °C), followed by short heat treatment (1h) and high heating rate, leads to smooth particle generation due to lower crystallinity of YAP phase (Regime II), Figure 4.

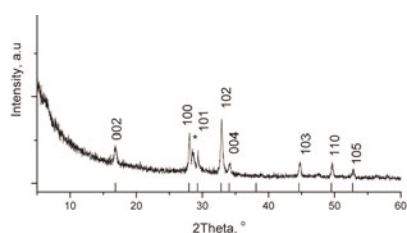


Figure 5. XRPD pattern of pure hexagonal YAP phase synthesized through spray pyrolysis at 900 °C, subsequently treated at 900 °C for 1h, Regime II (* - CeO₂)

The presence of the coarser (size ~ 1 μm) particles indicates change in mechanism of particle densification; higher heating rate decreases diffusion time during spray pyrolysis and averts further particle shrinkage. Although less visible at the surface, present porosity is sufficient one to prevent bursting of particle due to volatilization of gaseous products during precursor decomposition. No residual organic components were detectable during chemical analysis. For all samples EDS confirms high purity of particle and pre-defined cations ratio of Y:Al ~1:1 (insets in Figures 6, 7).

YAG phase: Figure 8 shows XRPD pattern of the sample obtained by spray pyrolysis of polymer precursor, containing Y:Al ratio of 3:5 (doped with 2 at.% of Ce) processed at 550 °C and heat treated at 1100 °C for 12h (Regime I). All diffraction lines can be readily indexed to pure cubic YAG structure with the space group *Ia-3d*. Table 3 presents refined crystal cell parameters together with the values of crystallite size and microstrains. All refinement-related data are given in Supplement file. Increase of the unit cell parameter and the Y-O bond lengths^[40] imply Ce³⁺ accommodation in garnet lattice. Still, partially substitution is established; CeO₂ formation is evident due to the detection of its reflections (111) and (220) in XRPD spectra.

Based on SEM images, presented at Figure 9, it is evident the influence of heat treatment at 1100 °C on particle morphology. Despite the fact that particles kept their spherical shape to a certain degree, prolonged heating time provokes their partial decomposition and stronger agglomeration. In principle, the particles are generated through volume precipitation and contain smaller grains, organised in pre-defined droplet spherical shape. Closer look of the grains on particle surface revealed their high crystallinity, Figure 10. The observed interplanar spacing

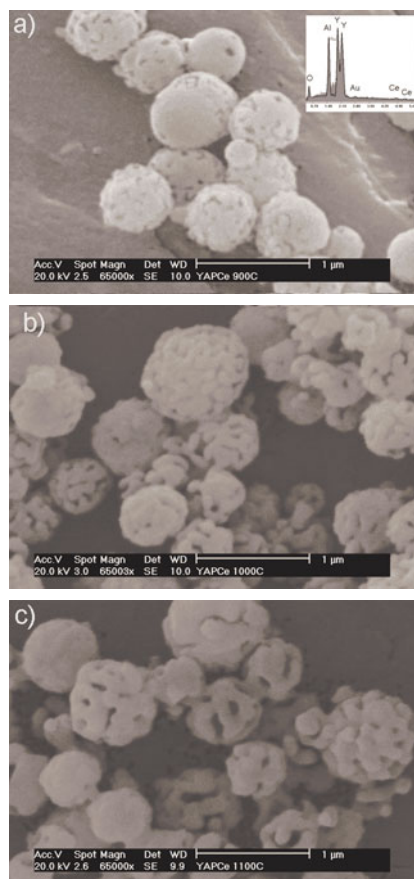


Figure 6. SEM/EDS analysis of particles synthesized from polymeric precursor solution (Y:Al=1) through spray pyrolysis at 550 °C and subsequently treated 12 h, Regime I at: 900 °C (a), 1000 °C (b), 1100 °C (c);

of 0.4251 Å (inset in Figure 10b) correlates well with the *d* value of (220) plane of the cubic YAG phase (0.4247 Å, JCPDS 33-0040). Continuous spreading of this plane through a whole grain, visible in Figure 10b, points to the fact that the subject grains are monocrystals.

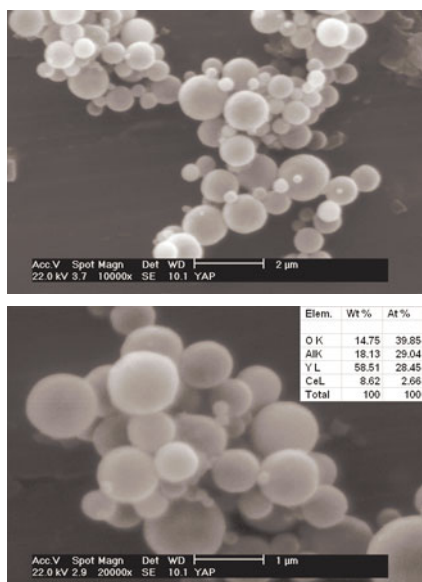


Figure 7. SEM analysis of particles synthesized from polymeric precursor solution (Y:Al=1) through spray pyrolysis at 900 °C subsequently treated at 1100 °C for 1 h, Regime II (inset presents result of semi-quantitative EDS analysis)

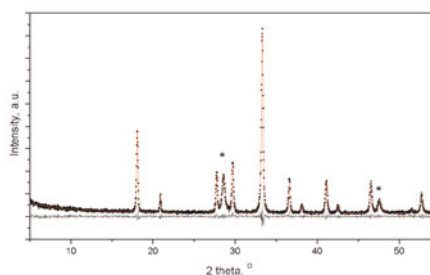


Figure 8. Rietveld refinement of XRPD pattern of pure cubic YAG phase synthesized through spray pyrolysis at 550 °C, subsequently treated at 1100 °C for 12h (* - CeO₂) Regime I

Table 3. The Rietveld refinement details and corresponding reliability factors for YAG:Ce³⁺ phase synthesized through spray pyrolysis at 550 °C and subsequently treated at elevated temperatures for 12 h (Regime I)

YAG:Ce ³⁺	
Space group	<i>Ia-3d</i>
a (Å)	12.0274(6)
Crystalite size (nm)	76(6)
Microstrain (%)	1.131(6)
R _{bragg} (%)	1.45
Goodnes of fit	1.062

As already indicated, among different yttrium aluminate phases, both the orthorhombic YAP and cubic YAG represent optically active materials when doped with Ce³⁺, having near-UV efficient emission. This emission originates from parity allowed electric dipole transitions between excited 5d and ground 4f states in Ce³⁺.

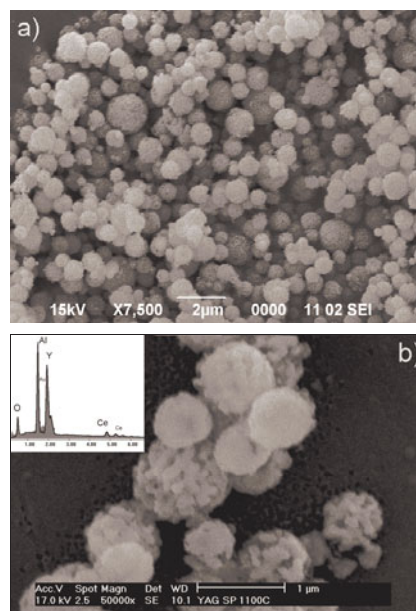


Figure 9. SEM/EDS analysis of particles synthesized from polymeric precursor solution (Y:Al=3:5) through spray pyrolysis at 550 °C, subsequently treated at: 1100 °C for 3 h (a), and 12h (b), Regime I

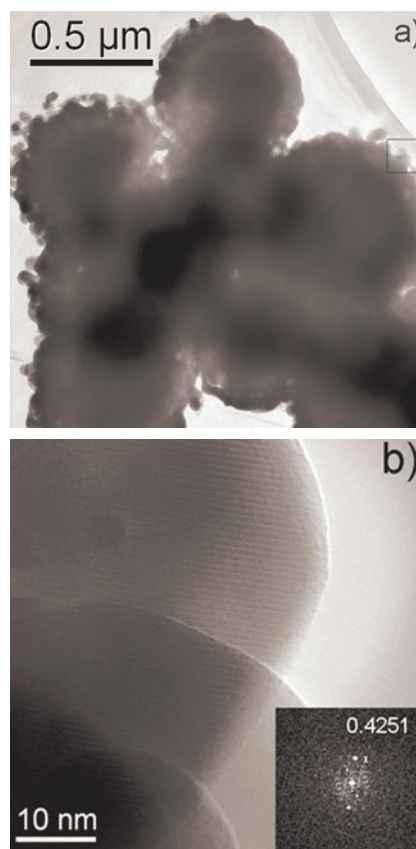


Figure 10. TEM/HR-TEM analysis of particles synthesized from polymeric precursor solution (Y:Al=3:5) through spray pyrolysis at 550 °C subsequently treated at 1100 °C for 3h, Regime I (Fast Fourier Transformation given in inset)

Due to crystal field effects, 5d orbitals have their energy levels divided into at least two sublevels- ²E and ²T₂, while due spin-orbit interactions, the lowest sublevels of 5d can be further split into new components, this also applies to ground state level 4f, split into the ²F_{5/2} and ²F_{7/2} components.^[6] When crystal field effect is strong,

the splitting of the 5d levels is so large that Ce^{3+} emission moves in the visible range. This is a case for garnet structure, which exhibits broad green-yellow emission band in the range of 500-650 nm. In contrast, orthorhombic YAP phase doped with Ce^{3+} , due its lower crystal field energy, emits the light at ~ 370 nm.^[23] The emission spectra recorded for the samples containing mixture of orthorhombic YAP and YAG phase (synthesized through spray pyrolysis at 550 °C and subsequently treated at elevated temperatures for 12 h, Regime I) are given in Figure 11. The recorded luminescence, peaking at $\lambda = 571$ nm, doubtlessly implies Ce^{3+} accommodation in garnet phase in all samples. No peaks are observed in the range typical for emission of $\text{YAP}:\text{Ce}^{3+}$ (inset in Figure 11), implying that regardless of the YAP/YAG phase content ratio, prolonged powder heating enhances Ce^{3+} accommodation in cubic crystal structure. Equality in luminescence intensity implies similar level of Ce^{3+} incorporation at yttrium position in garnet crystal unit. The afore-said can be also deduced from similar values of crystal unit parameter a , given in Table 2. At the same figure it is also present the spectra related to pure YAG phase synthesized through spray pyrolysis at 550 °C and subsequently treated at 1100 °C. More narrow and blue-shifted emission, peaking at 520 nm, can be also ascribed to the excited $^2\text{D}_j$ electron transition to the ground $^2\text{F}_{5/2,7/2}$ states. Observed change in emission wavelength could be a consequence of lower Ce^{3+} substitution in garnet lattice^[41], confirmed by smaller change of lattice parameter (a values for YAG in Tables 2, 3). Hence, better crystal cell arrangement (confirmed by HR-TEM) results in narrowing of the emission line in photoluminescence spectra.

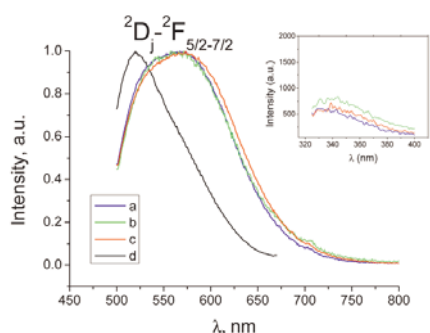


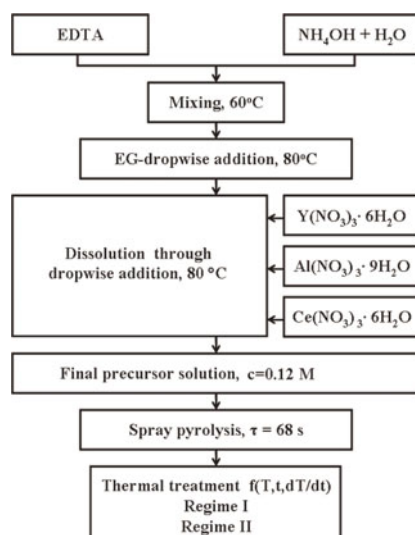
Figure 11. Photoluminescence emission spectra of particles synthesized from polymeric precursor solution (Y:Al=1) through spray pyrolysis at 550 °C and subsequently treated 12 h, Regime I, at: 900 °C (a), 1000 °C (b), 1100 °C (c); and from polymeric precursor solution (Y:Al=3:5) through spray pyrolysis at 550 °C and subsequently treated 3 h at 1100 °C, Regime I (d) ;

Conclusions

Highly spherical, un-agglomerated and dense particles of Ce^{3+} activated yttrium-aluminate phosphors are obtained via spray pyrolysis of polymeric precursor solution. Although positive, EDTA-EG introduction in common nitrate precursor is not sufficient for pure YAP phase generation. Namely, for predefined cations ratio, lower temperatures during spray pyrolysis combined with longer heat treatments in stationary conditions led to multi-phase system generation, while short processing at higher temperature associated with a high heating rate (200 °/min) during calcination results in stabilisation of kinetically favoured YAP hexagonal phase. Generation of the pure thermodynamically stable YAG phase is confirmed, regardless applied heat treatment conditions..

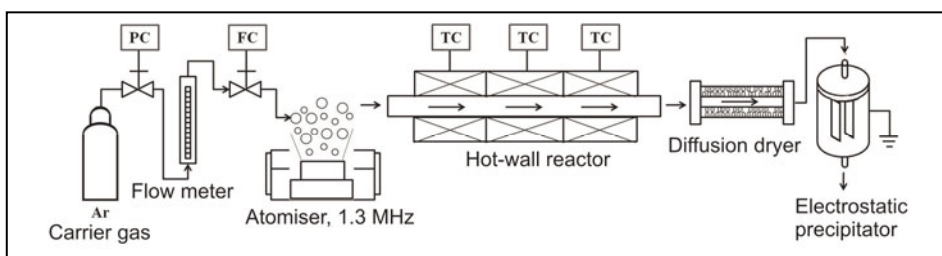
Experimental Section

Precursor preparation: Polymeric precursor solutions were prepared by application of yttrium nitrate ($\text{Y}(\text{NO}_3)_3 \cdot 6\text{H}_2\text{O}$, 99.9 %, Sigma-Aldrich), aluminium nitrate ($\text{Al}(\text{NO}_3)_3 \cdot 9\text{H}_2\text{O}$, 99.9 %, Sigma-Aldrich), cerium nitrate ($\text{Ce}(\text{NO}_3)_3 \cdot 6\text{H}_2\text{O}$, 99.9 %, Sigma-Aldrich), ethylenediaminetetraaceticacid $\text{C}_{10}\text{H}_{16}\text{N}_2\text{O}_8$ (EDTA) and ethylene glycol $\text{C}_2\text{H}_6\text{O}_2$ (EG) as starting materials. Yttrium and aluminum nitrates were mixed in appropriate molar ratio of 1:1 (for the synthesis of the YAP phase), and 3:5 (for the synthesis of the YAG phase). EDTA ratio to total metal ions was 1:1, while EDTA towards EG was 1:4. Cerium concentration ranged from 2 to 5 at.-%. The procedure of metal ions complexation and subsequent esterification was as follows: 0.1 mol EDTA was dissolved in ammonium hydroxide solution at 60 °C and after that slowly added to 0.4 mol EG while raising temperature to 80 °C. All the nitrates, were first separately dissolved in deionised water and then dropwise added to the main solution. Ammonium hydroxide was continuously added to prevent EDTA precipitation during salt addition; following the finalisation of the reaction, pH value was adjusted to 0.5 with the help of HNO_3 . There was no sign of precipitation in the course of the synthesis, but the colour of the solution changed to pale yellow. Synthesis procedure for polymer precursor preparation and powder processing is given on Scheme 1.



Scheme 1. Synthesis procedure for polymer precursor preparation and subsequent powder processing

Powder preparation: The prepared precursor solution was placed in a 1.3 MHz ultrasonic atomizer, wherefrom it was introduced, by means of carrier gas (Ar), in the form of aerosol into a hot-wall tubular reactor with three independent heating zones. The droplet/particle residence time (τ) in reactor was 68 s. In all experiments, the decomposition temperature was set to be either 550 °C or 900 °C for the YAP synthesis and 550 °C, for the YAG synthesis. The as-prepared powders were collected in electrostatic precipitator and additionally thermally treated at 900/1000/1100 °C either for 1, 3 or 12h in the air atmosphere. Two heating regimes were applied during thermal treatments in order to evaluate the phase stabilisation and to prevent the composite inhomogeneities; heating in a chamber furnace in stationary conditions (heating/cooling rates of approx. 6 °/min) (Regime I) and fast heating in a tubular furnace (heating rate of approx. 200 °/min) (Regime II). Experimental setup, used for spray pyrolysis, is given at Scheme 2.



Scheme 2. Experimental set-up for spray pyrolysis

Characterisation: Precursors compositional and structural changes during thermal decomposition were investigated by thermogravimetric and differential thermal analyses (TGA/DTA) and Fourier transform infrared emission spectroscopy (FTIR). TGA/DTA measurements have been performed on the SETARAM SET-SYS Evolution-1750 instrument at the heating rate of 10 °C/min. FTIR spectra were recorded at room temperature on Nicolet spectrophotometer (Model 380, Thermo Nicolet Corporation, Madison, USA). Powders phase identification was done by X-ray powder diffraction (XRPD), using X'Pert Philips diffractometer operating with Cu K_α radiation at 40mA and 40kV (data range: 5-100°; scan step: 0.02 °; time per step: 10 s). Fundamental Parameter Approach (FPA) in Topas Academic 4.1 software^[42] was applied for structure refinement; the background was refined using the sixth-order Chebichev function, while peak profile shapes were convoluted through Pawley (Lorentzian- and Gaussian-type for crystallite size and strain components) or Rietveld (predefined Double-Voigt approach for crystallite size) analysis. After the convergence, atomic positions and isotropic temperature factors were also included in the refinement. The particle's morphological features and chemical purity were investigated by means of scanning electron microscopy (Philips SEM XL30/EDS Dx4) and transmission electron microscopy (JEOL 2010 operating at 200 kV). For the scope of TEM analysis, the sample was prepared by ultramicrotomy, in compliance with the procedure as follows: small quantity of powder has been embedded in a resin and then cut to 90 nm thick foils in an ultramicrotome (Reichert-Jung). Steady state fluorescence was performed with an Edinburgh spectrofluorimeter. An optical fiber cable was used for exciting and collecting the fluorescence. In all cases the excitation and emission slits were set to be 5 mm. Excitation were done at 297 nm (YAP) and 450 nm (YAG). The recording of fluorescent response was completed in 325-800 nm range.

Supporting Information: <http://www.eurjic.org/>

Acknowledgments

The authors are grateful to the Ministry of Science and Education of the Republic of Serbia (Project No 172035) as well as the University Carlos III, Madrid, Spain- Santander Bank Chairs of Excellence program (academic year 2010-2011) for the financial support. The help of Dr. Dragana Jovanovic from Vinca Institute, Belgrade referred to FTIR analysis is highly appreciated.

[1] C.P. Khattak, F.F.Y. Wang, *Perovskites and garnets*, in *Handbook on the Physics and Chemistry of Rare Earths*, (Eds.: K.A. Gschneidner, Jr. and L. Eyring), North-Holland Publishing Company, **1979**, Vol 3, pp 525-607.

[2] K. Zhang, W. Hu, Y. Wu, H. Liu, *Ceram. Int.* **2009**, *35*, 719-723.

[3] B. Basavalingu, H.N. Girish, K. Byrappa, K. Soga, *Mater. Chem. Phys.* **2008**, *112*, 723-725.

[4] S. Mathur, H. Shen, R. Rapalaviciute, A. Kareiva, N. Donia, *J. Mater. Chem.* **2004**, *14*, 3259-3265.

[5] N. Kalivas, I. Valais, D. Nikolopoulos, A. Konstantinidis, A. Gaitanis, D. Cavouras, C.D. Nomicos, G. Panayiotakis, I. Kandarakis, *Appl. Phys. A Mater.* **2007**, *89*, 443-449.

[6] T.B. de Queiroz, C.R. Ferrari, D. Ulbrich, R. Doyle, A.S.S. de Camargo, *Opt. Mater.* **2010**, *32*, 1480-1484.

[7] D. Cao, G. Zhao, J. Chen, Q. Dong, Y. Ding, Y. Cheng, *J. Alloy. Compd.* **2010**, *489*, 515-518.

[8] J. Marchal, T. John, R. Baranwal, T. Hinklin, R.R. Laine, *Chem. Mater.* **2004**, *16*, 822-831.

[9] K.M. Kinsman, J. McKittrick, *J. Am. Ceram. Soc.* **1994**, *77*, 2866.

[10] S.M. Sim, K.A. Keller, T.I. Mah, *J. Mater. Sci.* **2000**, *35*, 713-717.

[11] A. Beltran, J. Andres, J. A. Igualada, J. Carda, *J. Phys. Chem.* **1995**, *99* (17), pp 6493-6501.

[12] M. Nyman, J. Caruso, M.J. Hampden-Smith, T.T. Kodas, *J. Am. Ceram. Soc.* **1997**, *80*, 1231-1238.

[13] C.K. Ullal, K.R. Balasubramaniam, A.S. Gandhi, V. Jayaram, *Acta Mater.* **2001**, *49*, 2691-2699.

[14] P.A. Tanner, P.T. Law, K.L. Wong, L. Fu, *J. Mater. Sci.* **2003**, *38*, 4857-4861.

[15] X. Guodong, Z. Shengming, Z. Junji, X. Jun, *J. Cryst. Growth*, **2005**, *279*, 357-362.

[16] S. Ramanathan, M.B. Kakade, S.K. Roy, K.K. Kutty, *Ceram. Inter.* **2003**, *29*, 477-484.

[17] J.G. Li, T. Ikegami, J.H. Lee, T. Mori, *J. Am. Ceram. Soc.* **2000**, *83*, 2866-2869.

[18] B. Basavalingu, H.N. Girish, K. Byrappa, K. Soga, *Mater. Chem. Phys.* **2008**, *112*, 723-725.

[19] M. Blosi, S. Albonetti, M. Dondi, A.L. Costa, M. Ardit, G. Cruciani, *J. Sol-Gel Sci Techn.* **2009**, *50*, 449-455.

[20] O. Milosevic, L. Mancic, M.E. Rabanal, J.M. Torralba, B. Yang, P. Townsend, *J. Electrochem. Soc.* **2005**, *152*, 707-713.

[21] Y. Wang, O. Milosevic, L. Gomez, M.E. Rabanal, J.M. Torralba, B. Yang, P.D. Townsend, *J. Phys. Condens. Matter*, **2006**, *18*, 9257-9272.

[22] D. Dosev, B. Guo, M.I. Kennedy, *Aerosol Sci. Tech.* **2006**, *37*, 402-412.

[23] M. Harada, A. Ue, M. Inoue, X. Guo, K. Sakuari, *Scripta Mater.* **2001**, *44*, 2243-2246.

[24] M. Harada, M. Goto, *J. Alloy. Compd.* **2006**, *408-412*, 1193-1195.

[25] J.F. Carvalho, F.S. De Vicente, N. Marcellin, P. Odier, A.C. Hernandez, A. Ibanez, *J. Therm Anal Calorim.* **2009**, *96*, 891-896.

- [26] J.F. Carvalho, F.S. De Vicente, S. Pairis, P.Odier, A.C. Hernandez, A. Ibanez, *J. Eur. Ceram. Soc.* **2009**, *29*, 2511-2515.
- [27] S. Wang, Y. Xu, P.Lu, C. Xu, W. Cao, *Mater. Sci. Eng. B*, **2006**, *127*, 203-206.
- [28] L. Mancic, K. Marinkovic, B.A. Marinkovic, M. Dramicanin, O. Milosevic, *J. Eur. Ceram. Soc.* **2010**, *30*, 577-582.
- [29] M. Galceran, M.C. Pujol, M. Aguilo, F. Diaz, *J Sol-Gel Sci Techn.* **2007**, *42*, 79-88.
- [30] L. Mancic, G. del Rosario, Z. Marinkovic, O. Milosevic, *Mater. Sci. Forum*, **2006**, *518*, 107-112.
- [31] J.F. Carvalho, F.S. De Vicente, N. Marcellin, P.Odier, A.C. Hernandez, A. Ibanez, *J Therm. Anal. Calorim.* **2009**, *96*, 891-896.
- [32] J.B. Zhang, K. Ma, F. Han, G.H. Chen, X.H. Wei, *Sci China Ser B-Chem.* **2008**, *51*, 5, 420-426.
- [33] X.H. Li, J.L. Dong, H.S. Xiao, P.D. Lu, Y.A. Hu, Y.H. Zhang, *Sci China Ser B-Chem*, **2008**, *51*, 2, 128-137.
- [34] G. Xia, S. Zhou, J. Zhang, J. Xu, *J Crystal Growth*, **2005**, *279*, 357-362.
- [35] M. Motta, C.V. Deimling, M.J. Saeki, P.N. Lisboa-Filho, *J Sol-Gel Sci. Technol.*, **2008**, *46*, 201-207.
- [36] A.Lukowiak, R.J. Wiglusz, m. Maczka, P. Gluchowski, W. Strek, *Chem Phys Lett.* **2010**, *494*, 279-283.
- [37] X.S. Jung, Y.K. Chung, D.M. Shin, S.D. Kim, *Bull. Chem. Soc. Japan*, **2002**, *75*, 1263-1267.
- [38] J.Wang, X.Zhang, Y. Zhang, Z. Liu, *WUJNS*, **2003**, *8*, 1131-1137.
- [39] C. Mao, L. Zhou, X. Wu, X. Sun, *Supercond. Sci. Technol.* **1996**, *9*, 994-1000.
- [40] F. Euler, J.A. Bruce, *Acta Crystallogr.* **1965**, *19*, 971-978.
- [41] Y.C. Kang, I.W. Lenggoro, S.B. Park, K.K. Okuyama, *Mater. Res. Bull.* **2000**, *35*, 789-798.
- [42] A.A.Coelho, *Topas –Academic*, **2006**.

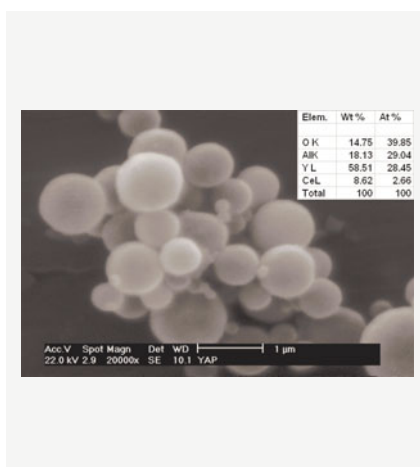
Received: ((will be filled in by the editorial staff))
 Published online: ((will be filled in by the editorial staff))

Entry for the Table of Contents

Layout 1:

((Key Topic))

Highly spherical, non-agglomerated polycrystalline YAP and YAG particles were synthesized via spray pyrolysis of the polymeric precursor solution. The presence of chelating agents enables pure YAP and YAG phase generation under the strictly defined thermal regime. Although incomplete, Ce^{3+} introduction into the host matrix is confirmed by XRPD and luminescence measurements.



Authors: Lidija Mancic, Vesna Lojpur, Ignacio Barosso, Maria Eugenia Rabanal and Olivera Milosevic*Page 1. – Page 7.

Title: Synthesis of cerium activated yttrium aluminate-based fine phosphors via aerosol route

Keywords: Yttrium aluminates / Nanoparticles/ Luminescence / Polymerization / Spray pyrolysis

Supporting Information

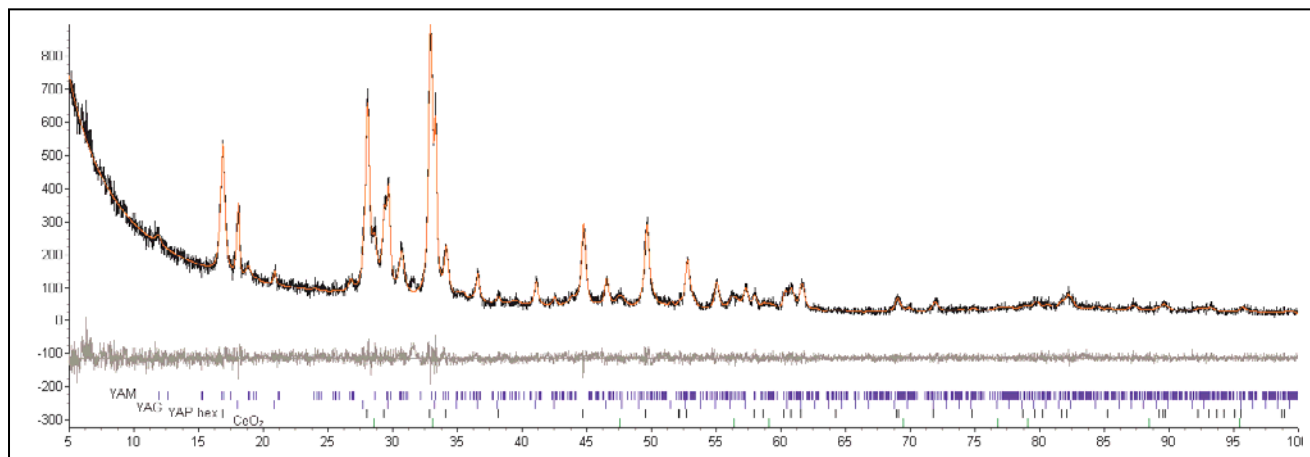


Figure S1. Topas^[42] output file for Pawley refinement of sample synthesized through spray pyrolysis of polymeric precursor solution (Y:Al=1) at 550 °C, subsequently treated at 900 °C for 12h; Regime I (in: black - collected data; red – calculated pattern; gray – difference curve; bars on the bottom relate to diffraction lines position for certain phases)

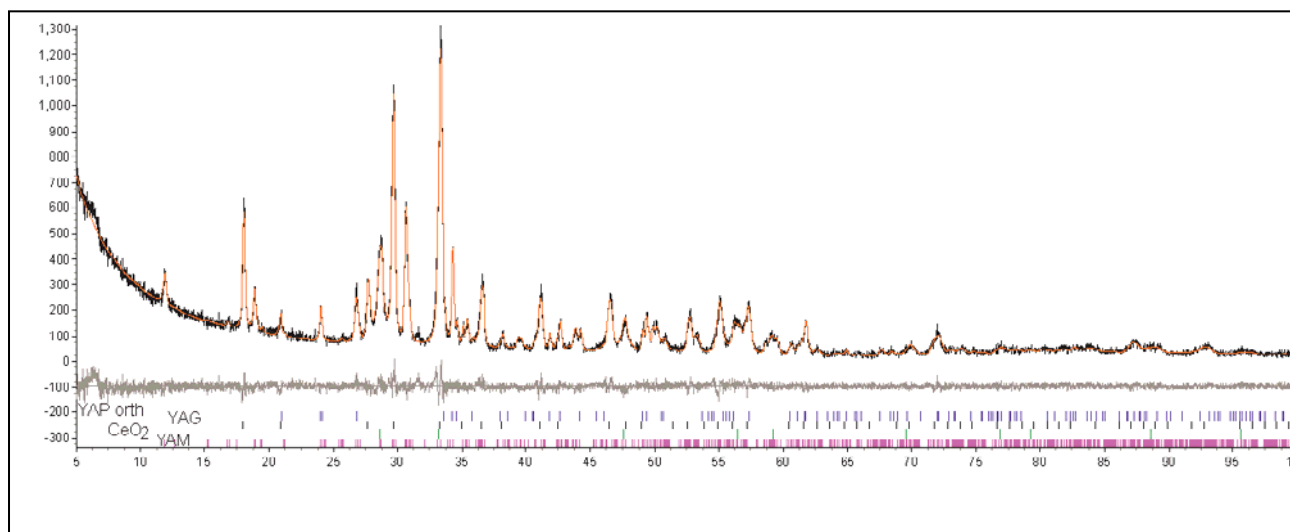


Figure S2. Topas^[42] output file for Pawley refinement of sample synthesized through spray pyrolysis of polymeric precursor solution (Y:Al =1) at 550 °C, and subsequently treated at 1000 °C for 12h; Regime I (in: black - collected data; red – calculated pattern; gray – difference curve; bars on the bottom are related to diffraction lines position for certain phases)

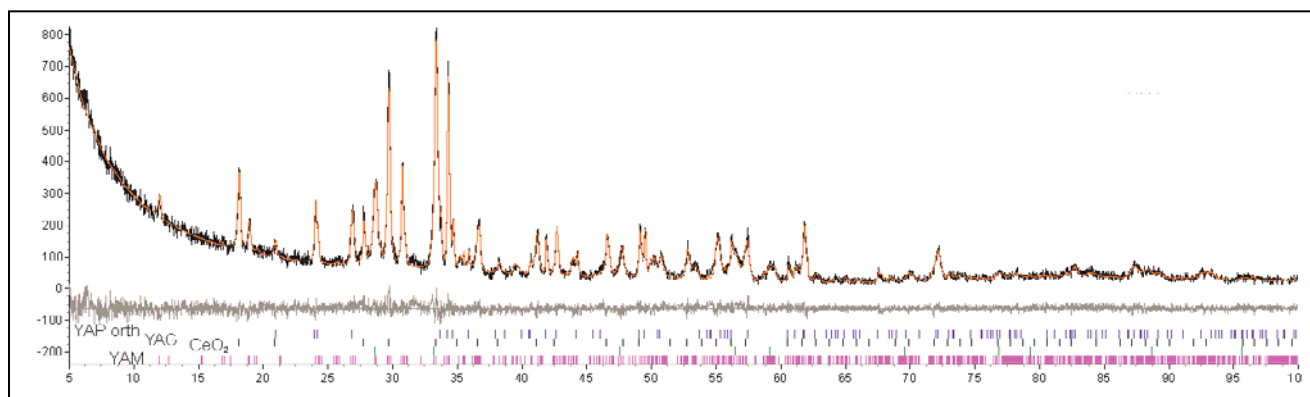


Figure S3. Topas^[42] output file for Pawley refinement of sample synthesized through spray pyrolysis of polymeric precursor solution (Y:Al=1) at 550 °C, subsequently treated at 1100 °C for 12h; Regime I (in: black - collected data; red – calculated pattern; gray – difference curve; bars on the bottom relate to diffraction lines position for certain phases)

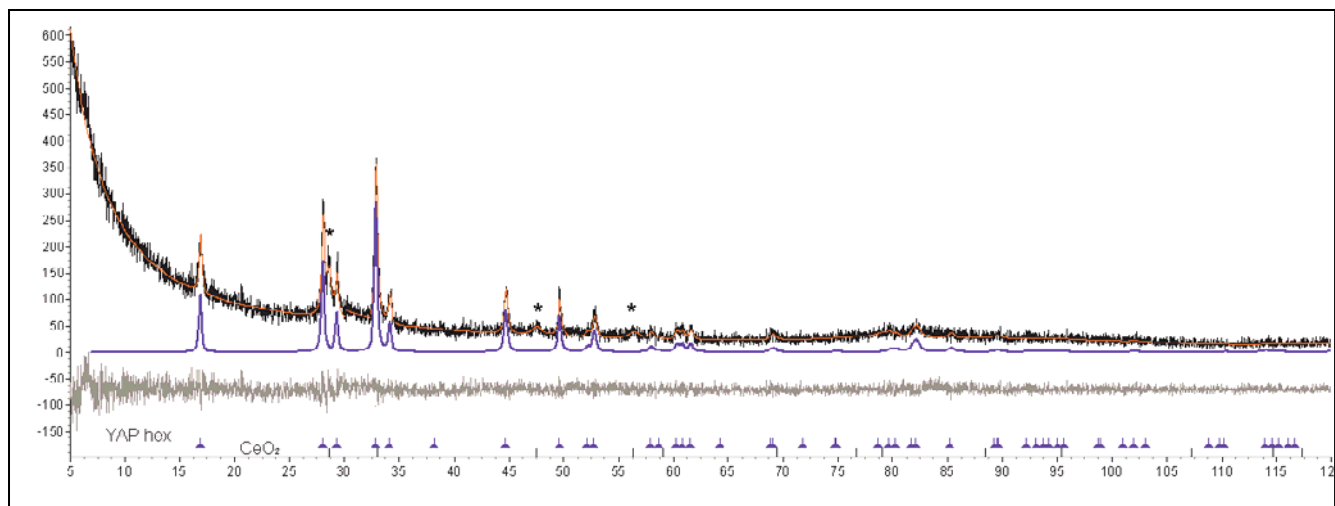


Figure S4. Topas^[42] output file for Pawley refinement of cubic YAP:Ce³⁺ phase synthesized through spray pyrolysis at 900 °C, subsequently treated at 900 °C for 1 h (* - CeO₂; in: black - collected data; red – calculated pattern; gray – difference curve; blue – refined YAP phase data; bars on the bottom relate to diffraction lines position for certain phases)

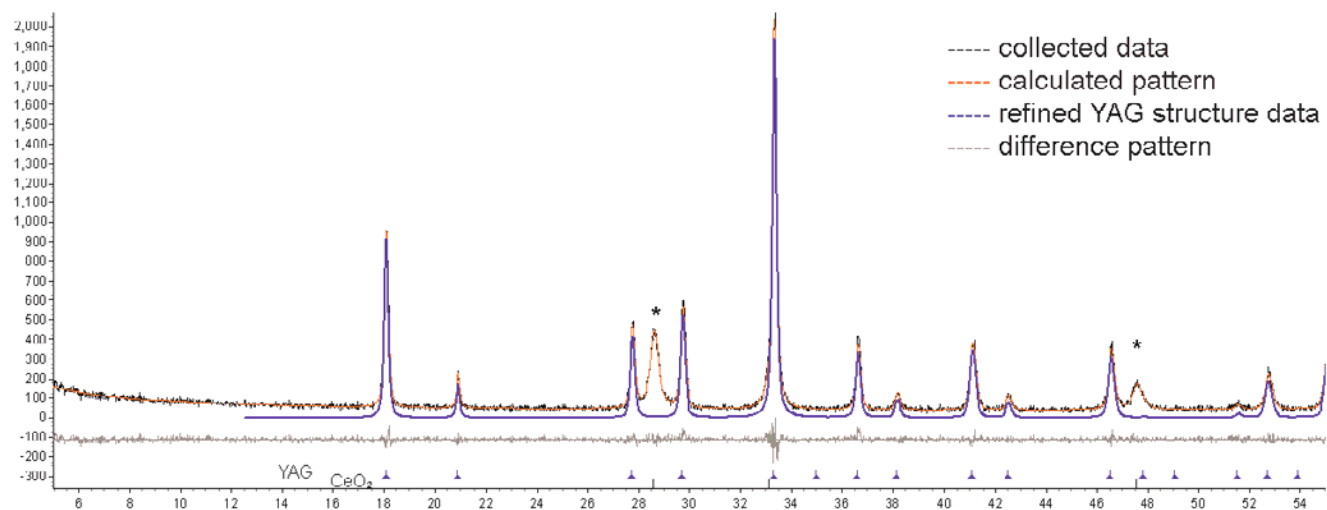


Figure S5. Topas^[42] output file for Rietveld refinement of cubic YAG:Ce³⁺ phase synthesized through spray pyrolysis at 550 °C, subsequently treated at 1100 °C for 12h (* -CeO₂, bars on the bottom relate to diffraction lines position for certain phases)

Table S1. Refined microstructural data for YAG:Ce³⁺ structure:

YAG:Ce ³⁺	
Space group	<i>Ia-3d</i>
a (Å)	12.02745_0.00063
Y coordinate:	
z	0.125
y	0
z	0.25
Al 1 coordinate:	
x	0
y	0
z	0
Al 2 coordinate:	
x	0.375
y	0
z	0.25
O coordinate:	
x	0.28089_0.00034
y	0.10093_0.00034
z	0.19998_0.00041
Bond distance (Å)	
Y-O2	2.3132(41)
Y-O1	2.4510(50)
Y-Al	3.00686
Crystalite size (nm)	76(6)
Microstrain (%)	1.131(6)
R _{bragg} (%)	1.45
R _{wp} (%)	11.007
R _{exp} (%)	10.362
Goodnes of fit	1.062
YAG ^[40] ; a=12 Å, bond distance (Å): Y-O ₂ : 2.303; Y-O ₁ : 2.432; Y-Al: 3.002;	

Subject: Acceptance 201101053 / Eur. J. Inorg. Chem.
From: eurjic@Wiley-VCH.de
Date: Thu, February 9, 2012 8:57 am
To: olivera.milosevic@itn.sanu.ac.rs
Cc: eurjic@Wiley-VCH.de

Subject: Acceptance 201101053 / Eur. J. Inorg. Chem.

Synthesis of cerium activated yttrium aluminate-based fine phosphors via aerosol route

DOI: 10.1002/ejic.201101053
for citing the article before print publication, please use this DOI number.

Dear Prof. Dr. Milosevic,

Thank you for the submission of your above-mentioned manuscript received on 03.10.2011. I am pleased to inform you that your revised Full Paper has now been finally accepted for publication in the European Journal of Inorganic Chemistry.

We have received your revised files safely and the separate graphic files as well. So we will now proceed with the processing of your paper. If there are any further questions we will contact you again.

Yours sincerely,

Dr. Karen J. Hindson
Editor, EurJIC
sent by Ursula Lerch (Editorial Assistant)

+++++

European Journal of Inorganic Chemistry

Postal Address:	Address for courier services:
Postfach 101161	Boschstr. 12
69451 Weinheim	69469 Weinheim
Germany	Germany

Tel (secretary): Int. code + 49 6201 606-255/359
Fax: Int. code + 49 6201 606203
e-mail: eurjic@wiley-vch.de
Homepage <http://www.eurjic.org/>

Tel: + 49 (0)6201 606255
Fax: + 49 (0)6201 606203
eurjic@wiley-vch.de
<http://www.eurjic.org>
Impact Factor (2010): 2.909
Co-owned and supported by ChemPubSoc Europe. (<http://www.chempubsoc.eu>)

Wiley-VCH Verlag GmbH & Co. KGaA
Location of the Company: Weinheim